REGULAR ARTICLE

blood advances

EMD originates from hyaluronan-induced homophilic interactions of CD44 variant-expressing MM cells under shear stress

Jiro Kikuchi,[1] Nobuyuki Kodama,[2,3] Masataka Takeshita,[2,3] Sho Ikeda,[4] Takahiro Kobayashi,[4] Yoshiaki Kuroda,[5] Michihiro Uchiyama,[6] Naoki Osada,[1] Bjarne Bogen,[7] Hiroshi Yasui,[8] Naoto Takahashi,[4] Akiyoshi Miwa,[2,3] and Yusuke Furukawa[1]

[1]Division of Stem Cell Regulation, Center for Molecular Medicine, Jichi Medical University, Tochigi, Japan; [2]Department of Hematology, Tokyo-Kita Medical Center, Tokyo, Japan; [3]International Myeloma Center for Advanced Research and Treatment, Japan Association for Development of Community Medicine, Tokyo, Japan; [4]Department of Hematology, Nephrology and Rheumatology, Akita University Graduate School of Medicine, Akita, Japan; [5]Department of Hematology, National Hospital Organization Hiroshimanishi Medical Center, Hiroshima, Japan; [6]Department of Hematology, Japanese Red Cross Society Suwa Hospital, Nagano, Japan; [7]Institute of Immunology, Oslo University Hospital, Oslo, Norway; and [8]Department of Hematology/Oncology, The Institute of Medical Science, University of Tokyo, Tokyo, Japan

Key Points

- Stromal cell–derived hyaluronan binds to CD44 variants on MM cells and generates cell clusters under shear stress in the bone marrow.
- MM cell clusters serve as a seed of EMD and express PI resistance-inducible genes upon release of CD44-intracellular domain.

Extramedullary disease (EMD) is known to be associated with chemoresistance and poor prognosis in multiple myeloma (MM); however, the mechanisms of its development are not fully understood. Elucidating the mechanism of EMD development and its therapeutic targeting would greatly contribute to further improvement of treatment outcome in patients with MM. Here, we show that bone marrow stroma cell–derived hyaluronan (HA) elicits homophilic interactions of MM cells by binding to surface CD44, especially long-stretch variants, under physiological shear stress and generates cell clusters that might develop into EMD. We recapitulated the development of EMD via administration of HA in a syngeneic murine MM model in a CD44-dependent manner. HA-induced MM cell clusters exhibited the specific resistance to proteasome inhibitors (PIs) in vitro and in murine models via γ-secretase–mediated cleavage of the intracellular domains of CD44, which in turn transactivated PI resistance-inducible genes. Treatment of HA-injected mice with anti-CD44 antibody or γ-secretase inhibitors readily suppressed the development of EMD from transplanted MM cells and significantly prolonged the survival of recipients by overcoming PI resistance. The HA-CD44 axis represents a novel pathway to trigger EMD development and could be a target of the prediction, prevention, and treatment of EMD in patients with MM.

Introduction

Multiple myeloma (MM) is the second most common hematologic malignancy, accounting for approximately 7% of newly diagnosed cancers globally.[1] Its worldwide incidence has increased steadily over the past 30 years due to global changes in age distribution and a higher prevalence of MM in older people. The treatment outcome of patients with MM has been significantly improved by the introduction of novel therapeutic agents, including proteasome inhibitors (PIs) and immunomodulatory drugs.[2] However, most patients eventually become resistant to treatment, and nearly half of the patients relapse and die of the disease within 5 years of diagnosis.[3] Therefore, novel treatment strategies based on a better understanding of MM biology are required to overcome drug resistance and improve quality of life, especially in older patients.

Submitted 10 February 2022; accepted 18 July 2022; prepublished online on *Blood Advances* First Edition 5 August 2022; final version published online 16 February 2023. https://doi.org/10.1182/bloodadvances.2022007291.

Data have been deposited in the MIAME-compliant Gene Expression Omnibus database under accession number GSE189364. For other data sharing, contact the corresponding author, Yusuke Furukawa (furuyu@jichi.ac.jp).

The full-text version of this article contains a data supplement.

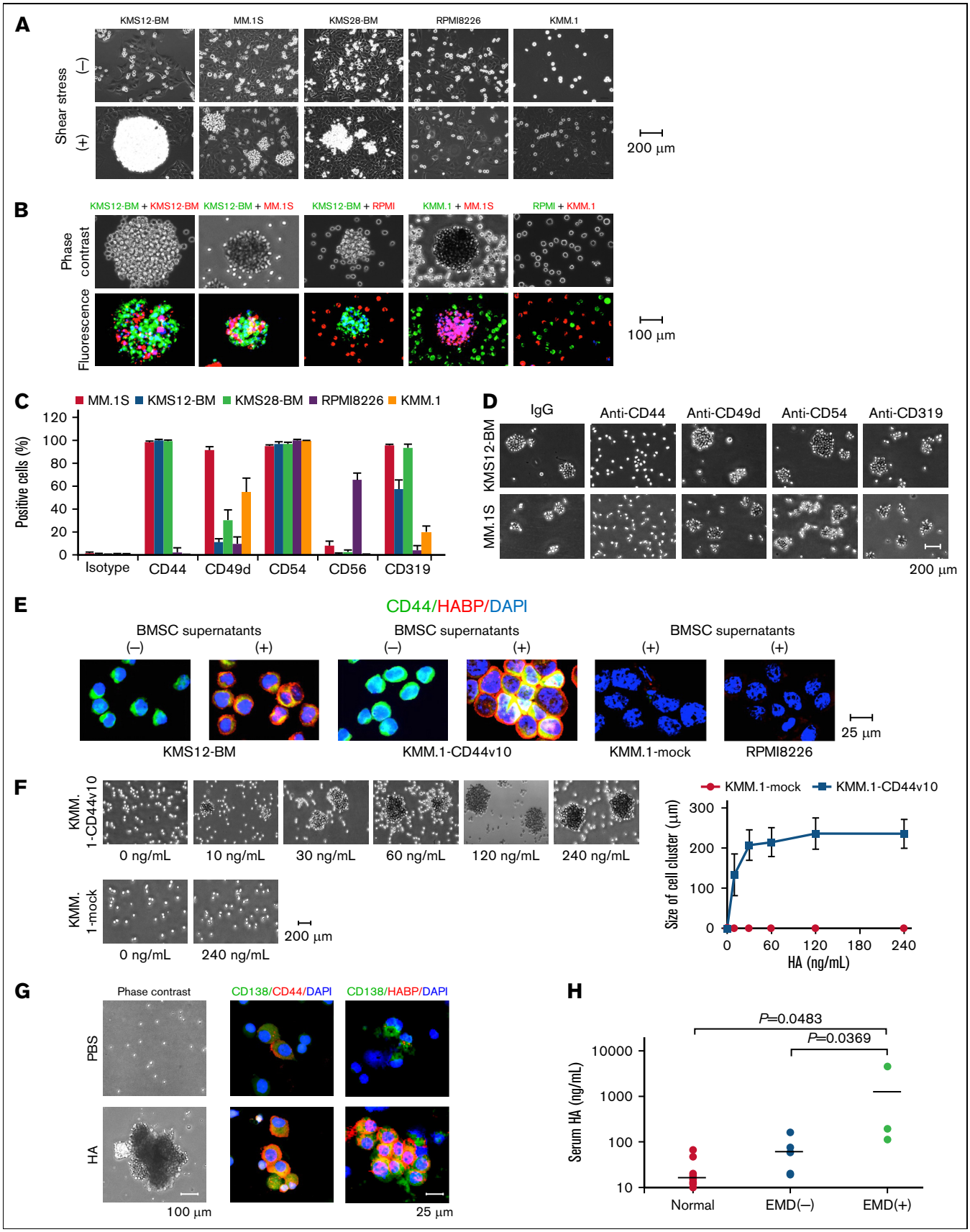

Figure 1.

MM is tumor derived from terminally differentiated B lymphocytes and usually resides in the bone marrow (BM), reflecting the nature of normal counterparts.[4] However, a subset of patients with MM present with extramedullary disease (EMD) characterized by the emergence of MM cells at anatomic sites distant from the BM, such as the liver (11.8% to 28.8%), spleen (0.8% to 11.5%), lymph nodes (17.3% to 23.1%), soft tissue/skin (11.1% to 29.1%), pleura/lung (2.7% to 25.0%), and central nervous system (3.0% to 11.0%).[5-7] EMD could be present at both diagnosis and relapse with incidences of 3% to 5% and 6% to 20%, respectively, depending on the definition.[8,9] EMD is a hallmark of dismal prognosis independent of other high-risk factors, particularly when it appears at the time of relapse.[10,11] The median survival of patients relapsed with EMD was reported to be only 5 months, even in the era of novel therapeutic approaches.[12] The mechanisms of EMD development should be elucidated to further improve the life expectancy of patients with MM, but they remain poorly explored thus far.

MM cells express various adhesion molecules, such as CD29 (β1-integrin), CD44, CD49d (β4-integrin, a subunit of VLA-4), CD49e (β5-integrin, a subunit of VLA-5), CD54 (ICAM-1), CD56 (NCAM), CD138 (syndecan-1), CD184 (CXCR4), and CD319 (SLAMF7), which play redundant roles in interacting with the BM microenvironment, and can promote drug resistance, cell growth, and functional activation.[13-17] It is reasonable to speculate that deregulation and/or dysfunction of adhesion molecules is involved in the migration of BM MM cells to extramedullary sites during EMD development. In fact, previous clinical studies revealed that MM cells isolated from EMD lesions displayed an increase in CD44 expression and reduced expression of VLA-5 and CD56.[18] Furthermore, the instructive roles of CXCR4, VLA-4, and P-selectin glycoprotein ligand-1 in EMD development have been demonstrated in murine MM models.[19,20] However, it is still unclear how these changes are mechanistically implicated in the development of EMD and whether they could be therapeutically targeted for clinical translation.

CD44 is a family of glycoproteins that share a standard form (CD44s) encoded by 10 exons as a common backbone. Several isoforms are generated via alternative splicing of 1 or more variable exons (v1-v10), resulting in the introduction of additional stretches in the extracellular stem region of CD44s.[21] In solid cancers, the extracellular domain of CD44 can either bind to hyaluronan (HA) or homotypically interact with another CD44 molecule to promote tumor progression and metastasis via cell–cell and/or cell–extracellular matrix interactions.[22-24] It was reported that CD44 and its variants were highly expressed in MM cells derived from patients with EMD[25,26] and that CD44 variant 9 (CD44v9) expression was a worse prognostic factor for patients with MM.[18,25] Moreover, serum HA concentrations were much higher in patients with MM than in healthy individuals and were significantly correlated with disease activity and treatment refractoriness in patients with MM.[27] Despite these clinical correlations, the involvement of the HA-CD44 axis in the development of EMD has not yet been fully investigated. In the present study, we show that HA-induced homophilic cell–cell interactions through CD44 variants represent an initial step of EMD development. This finding might be translated to the clinic for the prediction, prevention, and treatment of EMD in patients with MM.

Methods

Cells and cell culture

The human myeloma cell lines MM.1S, KMS12-BM, KMS26, KMS28-BM, U266, KMM.1, and RPMI8226 were purchased from the Health Science Research Resources Bank (Osaka, Japan), where the cell line authenticity and absence of *Mycoplasma* infection are routinely checked by DNA fingerprinting and polymerase chain reaction (PCR) and maintained in RPMI1640 medium supplemented with 10% heat-inactivated fetal bovine serum (FBS). The human BM-derived stromal cell lines UBE6T-7 and stroma-NK, which were immortalized by transduction with a human telomerase catalytic protein subunit,[28,29] were maintained in 10% FBS-containing Dulbecco's Modified Eagle Medium and used as BM stromal cells (BMSCs) after changing the culture medium to 10%

Figure 1. HA promotes cluster formation of CD44$^+$ MM cells under shear stress. (A) The indicated MM cells were cultured at 1 to 5 × 10^5 cells/mL on a feeder layer of UBE6T-7 BMSCs with or without exposure to shear stress for 1 hour. We continuously rotated 25 cm^2 culture flasks at 60 rpm on a horizontal rotator to generate 10 dyne/cm^2 shear force, which is virtually identical to the force from blood flow in the BM.[32,33] Representative phase-contrast images of MM cells are shown. Bar represents 200 μm. (B) The indicated MM cell lines were prestained with green or red MitoTracker, as indicated, and cultured at a 1:1 ratio in the presence of the supernatant from UBE6T-7 cells for 1 hour under shear stress. Representative phase-contrast images and fluorescence images are shown in the upper and lower panels, respectively. Nuclei were counterstained with DAPI (blue). Bar represents 100 μm. (C) Flow cytometric analysis of the expression of adhesion molecules on MM cells. The means ± SD (bars) of 3 independent experiments are shown. Isotype/isotype-matched controls. (D) KMS12-BM and MM.1S cells were treated with 100 μg/mL of isotype-matched immunoglobulin (IgG) or specific antibodies against CD44, CD49d, CD54, or CD319/SLAMF7 in the presence of UBE6T-7 supernatants for 2 hours, followed by 1-hour culture under shear stress. Representative phase-contrast images are shown. Bar represents 200 μm. (E) KMM.1 cells transduced with an empty vector (KMM.1-mock) or CD44v10-expression vector (KMM.1-CD44v10) were cultured in the absence or presence of UBE6T-7 supernatant for 1 hour under shear stress. KMS12-BM and RPMI8226 cells were cultured under the same conditions as positive and negative controls, respectively. Cytospin specimens were stained with anti-CD44 antibody and biotin-conjugated HABP followed by staining with Alexa Fluor 488-conjugated anti-mouse IgG (green) and Alexa Fluor 594-conjugated streptavidin (red). Nuclei were counterstained with DAPI (blue). Bar represents 25 μm. (F) Left panel: KMM.1-mock or KMM.1-CD44v10 cells were treated with HA at the indicated concentrations for 1 hour without BMSC supernatants under exposure to shear stress. Representative phase-contrast images are shown. Bar represents 200 μm. Right panel: The means ± SD (bars) of the cell cluster sizes are shown (n = 10-20). (G) Mononuclear cells isolated from EMD lesions of patients with MM were cultured with phosphate-buffered saline (PBS) or 500 ng/mL of HA for 1 hour under shear stress. Left panel: Representative phase-contrast images. Bar represents 100 μm. Right panel: Cytospin specimens were stained with FITC-conjugated anti-CD138 antibody (green) and PE-conjugated anti-CD44 antibody (red) or biotin-conjugated HABP, followed by staining with Alexa Fluor 594-conjugated streptavidin (red) and DAPI (blue). Bar represents 25 μm. (H) Serum HA concentrations in normal healthy volunteers (Normal) (n = 10), patients with MM without EMD [EMD (–)] (n = 5), and patients with MM with EMD [EMD (+)] (n = 3) were measured with an enzyme-linked immunosorbent assay. Bars indicate the means of each group. **P* values were determined by one-way analysis of variance (ANOVA) with Tukey's multiple comparison test.

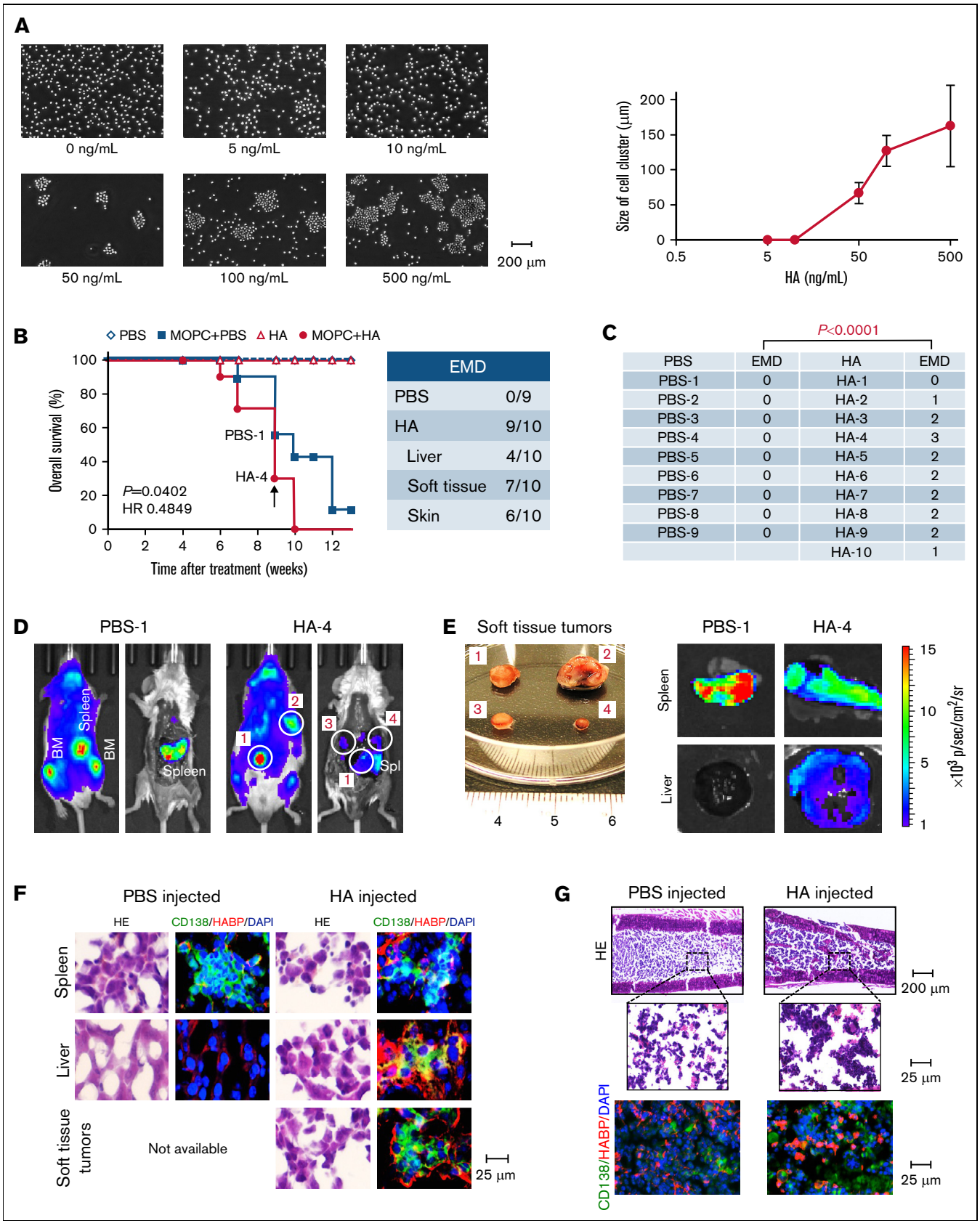

Figure 2.

FBS-RPMI1640. BMSC culture supernatants were prepared from confluent UBE6T-7 and stroma-NK cells cultured in fresh 10% FBS-RPMI1640 for 24 hours. For coculture experiments, BMSCs were cultured in a 25 cm^2 flask until reaching >90% confluence, and then MM cells were seeded on the layer of BMSCs. To generate shear force, culture flasks were continuously rotated at 0 to 120 rpm on a horizontal orbital shaker in a humidified atmosphere of 5% CO_2 at 37°C. Primary BM cells were isolated from patients with MM at the time of the diagnostic procedure and used with or without positive selection of MM cells using CD138 MicroBeads and MACS separation columns (Miltenyi Biotech, Bergisch Gladbach, Germany). We obtained written informed consent from all patients in accordance with the Declaration of Helsinki. The protocol was approved by the Institutional Review Boards of Jichi Medical University, Tokyo-Kita Medical Center, Akita University Graduate School of Medicine, Hiroshima-Nishi Medical Center, and Japanese Red Cross Society Suwa Hospital.

Construction and production of lentiviral expression vectors

We used the lentiviral vector CSII-CMV-MCS-IRES-VENUS (provided by Hiroyuki Miyoshi, RIKEN BioResource Center, Ibaraki, Japan) containing the coding regions of *CD44s*, *CD44v6*, *CD44v9*, and *CD44v10* cDNA for gain-of-function experiments. We used a lentiCRISPRv2 vector which expresses gRNA and Cas9 nuclease for CRISPR/Cas9-mediated deletion of target genes (Addgene, Cambridge, MA). Each sequence of the CRISPR targets was designed using the CRISPRdirect tool (http://crispr.dbcls.jp/) and is shown in supplemental Table 1.

Global analysis of mRNA expression

Total cellular RNA was isolated from MM.1S and KMS12-BM cells cultured in the presence of UBET6T-7 culture supernatants with or without shear stress for 24 hours. RNA samples (50 ng) were T7-primed and reverse-transcribed, followed by T7 transcription in the presence of Cy3- (for RNA from cells cultured without shear stress) or Cy5-CTP (for RNA from cells exposed to shear stress). Labeled cRNAs were hybridized with the SurePrint G3 Human Gene Expression 8 × 60K version 3.0 Microarray (Agilent Technologies, Santa Clara, CA). The hybridized arrays were scanned on an Agilent G2505C Scanner, and the scanned images were processed using the Agilent Feature Extraction software (version 12.0.3.1).

Xenogeneic and syngeneic murine MM models

For ex vivo tracing of tumors, we established luciferase-expressing sublines of KMM.1 and MOPC315.BM, designated KMM.1-Luc and MOPC315.BM.Luc, respectively, by transfecting firefly luciferase cDNA into the parent lines.[15,30] KMM.1-Luc cells were suspended in 100 μL of RPMI 1640 medium and subcutaneously inoculated in the right thigh of male nonobese diabetic/severe combined immunodeficiency (NOD/SCID) mice (Charles River Laboratories, Wilmington, MA).[16] MOPC315.BM.Luc cells were suspended in 100 μL of RPMI 1640 medium and injected intravenously into male BALB/c mice (Charles River Laboratories). Drugs were administered intraperitoneally in a 200-μL volume of solution containing 5% dimethyl sulfoxide (vol/vol) in sterile phosphate-buffered saline. The control group received the vehicle alone on the same schedule. Tumor burden was monitored by measuring tumor-derived luciferase activity with a noninvasive bioimaging system. In short, tumor-bearing mice were intraperitoneally injected with 1.5 mg of the luciferase substrate *D*-luciferin after being anesthetized with isoflurane. Photons transmitted through the body were collected for a specified length of time and analyzed using the IVIS-CT Imaging System with Living Image software (Xenogen, Alameda, CA). Quantitative data were expressed as photon units (photons/s). All animal studies were approved by the Institutional Animal Ethics Committee and were performed in accordance with the Guide for the Care and Use of Laboratory Animals formulated by the National Academy of Sciences.

Other conventional techniques and reagents used in this study are described in supplemental Data.

Results

HA promotes cluster formation of $CD44^+$ MM cells under shear stress

Recent studies suggest that the risk of EMD development is largely dependent on the intrinsic ability of MM cells, such as the presence of cytogenetic abnormalities and alterations in adhesion molecules, in the BM microenvironment.[31] To understand the initial step of EMD development, we recreated the BM microenvironment by cultivating MM cells on a feeder layer of BMSCs under shear stress, an overlooked but important determinant of cell fate. Hematopoietic cells are constantly exposed to shear stress at 2.5 to 20 dyne/cm^2 from blood flow in BM venules.[32,33] We rotated

Figure 2. The administration of HA facilitates EMD development in a syngeneic murine MM model. (A) MOPC315.BM-Luc cells were cultured at 1 × 10^5 cells/mL with various concentrations of HA under shear stress for 1 hour. Left panel: Representative phase-contrast images at the indicated concentrations of HA. Bar represents 200 μm. Right panel: The means ± SD (bars) of cell cluster sizes (n = 8-20). (B) We intravenously injected 5 × 10^5 luciferase-expressing MOPC315.BM.Luc cells or vehicle alone (PBS) into BALB/c mice, started the administration of the vehicle (PBS) or 50 μg/kg of HA 4 weeks after transplantation, and continued the treatments twice a week for an additional 4 weeks. Kaplan-Meier survival curves of the PBS group (PBS-injected and PBS-administered mice) (n = 5), the MOPC + PBS group (MOPC315.BM.Luc-transplanted and PBS-administered mice) (n = 9), the HA group (PBS-injected and HA-administered mice) (n = 5), and the MOPC + HA group (MOPC315.BM.Luc-transplanted and HA-administered mice) (n = 10). *P* values and the hazard ratio (HR) were determined between the MOPC + PBS group and the MOPC + HA group by the log-rank test. (C) The numbers of EMD lesions in each mouse were counted. The *P* value was determined by Student *t* test. (D) Representative photographs of whole-body ventral images obtained by the IVIS Imaging System on Day 63 (indicated by an arrow in B) before and after euthanasia in the left and right panels, respectively (original magnification, ×2). Luciferase-expressing soft tissue tumors are circled and numbered. (E) Representative photographs and ex vivo images of soft tissue tumors, designated #1 to approximately #4 in D, spleen, and liver resected from the PBS-1 and HA-4 mice (original magnification, ×2). See supplemental Figure 3D for all mice and supplemental Figure 3F for quantification. (F) Spleen, liver, soft tissue tumors, and (G) BM sections were obtained from mice in D and stained with hematoxylin-eosin (HE) or with FITC-conjugated anti-human CD138 antibody (green) and biotin-conjugated HABP, followed by the staining with Alexa Fluor 584-conjugated streptavidin (red) and DAPI (blue).

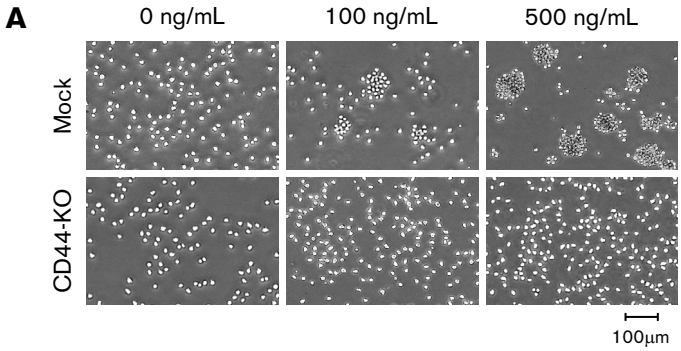

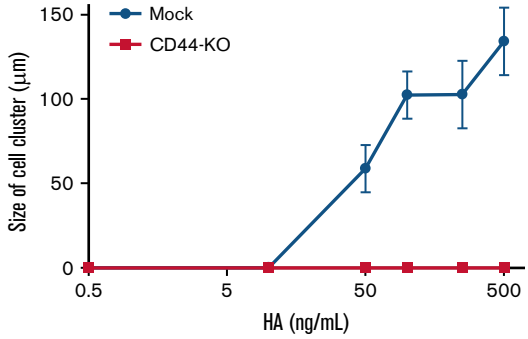

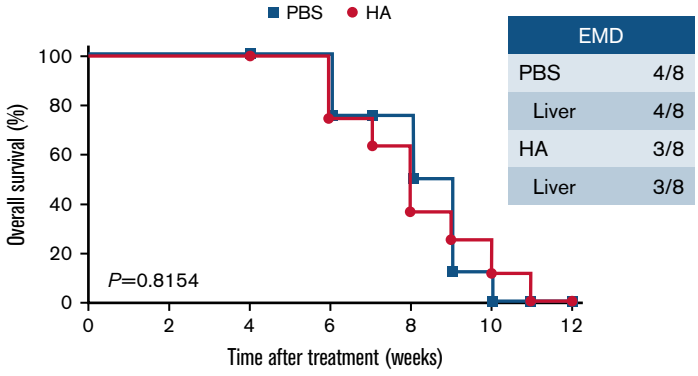

EMD	
PBS	4/8
Liver	4/8
HA	3/8
Liver	3/8

C

P=0.64

PBS	EMD	HA	EMD
#1	1	#1	0
#2	0	#2	1
#3	1	#3	0
#4	0	#4	0
#5	1	#5	1
#6	0	#6	0
#7	1	#7	1
#8	0	#8	0

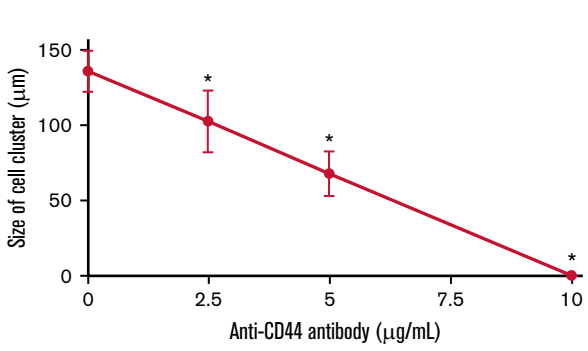

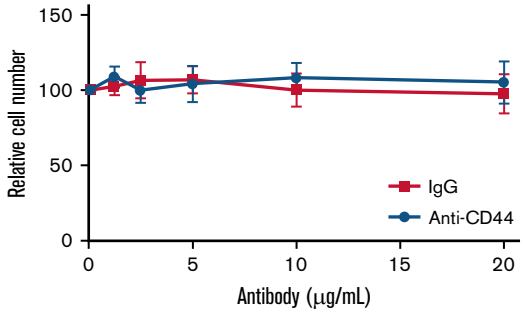

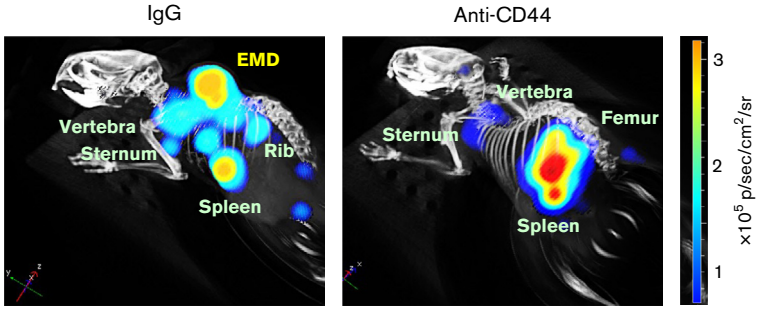

G

P=0.02191

IgG	EMD	Anti-CD44	EMD
#1	1	#1	0
#2	1	#2	2
#3	1	#3	0
#4	2	#4	1
#5	1	#5	0
#6	1	#6	0
#7	1	#7	0
#8	3	#8	1

Figure 3.

culture flasks at 60 rpm on a horizontal rotator, which generates 10 dyne/cm^2, to reproduce physiological shear stress in vitro. Among the 5 MM cell lines used in this study, KMS12-BM, MM.1S, and KMS28-BM cells dissociated from the BMSC lines UBE6T-7 and stroma-NK and interacted with each other to generate cell clusters up to 500 μm in size, whereas RPMI8226 and KMM.1 cells did not form clusters under the same conditions (Figure 1A; supplemental Figure 1A). Culture supernatants of BMSCs similarly induced the formation of MM cell clusters, suggesting that BMSC-derived soluble factors, including MM cell-stimulatory cytokines interleukin-6 and insulin-like growth factor-1 as well as HA,[13] are responsible for this process (supplemental Figure 1B). Supernatant-induced cluster formation was observed under physiological ranges of shear force (supplemental Figure 1C).

Mixed culture experiments revealed that KMS12-BM and MM.1S cells were able to form mixed clusters, but RPMI8226 and KMM.1 cells failed to do so, suggesting that cluster formation depends on specific adhesion molecule(s) (Figure 1B). Among the major adhesion molecules, CD44 and CD319/SLAMF7 were correlated with the ability of cluster formation of MM cells (Figure 1C). A specific antibody against CD44, but not against CD49d, CD54, or SLAMF7, abrogated cell cluster formation (Figure 1D). A major ligand of CD44, HA,[34] was produced by BMSCs but not MM cells at a considerable amount (500-1500 ng/mL); this probably occurred through HAS3, 1 of 3 HA-synthesizing enzymes (supplemental Figure 1D/E). An HA nonproducing BMSC, BJ,[35] did not promote MM cluster formation (supplemental Figure 1A) and lacks HAS3 expression (supplemental Figure 1D/E). Indeed, immunofluorescent staining with HA-binding protein (HABP) clearly detected HA on the surface of cell clusters derived from CD44$^+$ KMS12-BM and CD44v10-transduced KMM.1 cells but not on clusters from CD44$^-$ RPMI8226 or mock-transfected KMM.1 cells cultured with BMSC supernatants (Figure 1E; supplemental Figure 1F). HA alone promoted cell cluster formation in CD44v10-transduced but not mock-transfected KMM.1 cells at concentrations >10 ng/mL and increased the size of clusters in a dose-dependent manner (Figure 1F). Other BMSC-derived humoral factors, such as interleukin-6 and insulin-like growth factor-1, did not generate cell clusters in MM.1S or RPMI8226 cells (supplemental Figure 1G).

Next, we confirmed HA-mediated cluster formation in primary MM populations, including those derived from EMD lesions. HA-induced cluster formation was observed with primary cells from BM and EMD lesions of patients with MM with EMD but not from MM cells from patients without EMD (Figure 1G; supplemental Figure 2A). EMD-derived cell clusters had elevated expression of CD44, whose engagement with HA was visualized by HABP staining (Figure 1G), compared with that in primary cells from patients without EMD (supplemental Figure 2B). In addition, serum HA concentrations were significantly higher in patients with MM with EMD than in those without EMD in a cohort of patients admitted to Tokyo-Kita Medical Center and Akita University Hospital (Figure 1H). An increase in serum HA concentrations preceded the development or worsening of EMD in representative patients in the cohort (supplemental Figure 2C-D). These results suggest that HA bridges MM cells via surface CD44, followed by expansion of bridged MM cells under shear stress, leading to cluster formation. Recent literature points to the association of circulating tumor clusters with metastasis of breast cancer[36] or dissemination of MM cells to extramedullary tissues.[37] Hence, it is highly likely that cluster formation represents an origin of EMD and provides mechanistic insight into EMD development in MM.

The administration of HA facilitates EMD development in a syngeneic murine MM model

Having demonstrated the role of HA in MM cluster formation, we attempted to recapitulate EMD in vivo using a murine model in which MOPC315.BM.Luc (MOPC) murine MM cells were injected intravenously into syngeneic BALB/c mice. In this model, MOPC cells engraft in the BM of long bones (skull, vertebra, sternum, femur, and tibia) and the spleen, another major hematopoietic organ in the mouse.[15,30] As observed in human MM cell lines, HA triggered the formation of MOPC cell clusters at >50 ng/mL in vitro and increased the cluster size in a dose-dependent manner (Figure 2A). Serum HA concentrations were <50 ng/mL in BALB/c mice even 8 weeks after engraftment of MOPC cells, which are not capable of producing HA (supplemental Figure 3A-B). The concentrations increased to >200 ng/mL after administration of 50 μg/kg of HA (supplemental Figure 3A-B); therefore, we decided to inject this dose of HA twice a week to supply a sufficient amount of HA to trigger cell cluster formation in vivo. When MOPC-derived luciferase activity was detected (usually 4 weeks after transplantation), we started intravenous injection of vehicle (phosphate-buffered saline) or HA and continued the procedure until humane endpoints such as an inability to consume food and water or marked weight loss. Whole-body imaging detected numerous luciferase-expressing masses at various sites outside the BM and spleen in HA-treated

Figure 3. CD44 is required for HA-induced cluster formation in vitro and EMD development in a mouse MM model. (A) We established MOPC315.BM-Luc sublines, in which CD44 was deleted using the CRISPR/Cas9 system (CD44-KO) or an empty vector was stably transfected (Mock). Mock and CD44-KO cells were cultured at 1 × 10^5 cells/mL with various concentrations of HA under shear stress for 1 hour. Left panel: Representative phase-contrast images of MM cells. Bar represents 100 μm. Right panel: The means ± SD (bars) of the size of cell clusters (n = 8-20). (B) We intravenously injected 5 × 10^5 CD44-KO cells into BALB/c mice, started the administration of the vehicle (PBS) or 50 μg/kg of HA 4 weeks after transplantation, and continued the treatments twice a week for an additional 4 weeks. Kaplan-Meier survival curves of the PBS group (n = 8) and the HA group (n = 8). *P* values were determined by the log-rank test. (C) The numbers of EMD lesions in each mouse were counted. The *P* value was determined by Student *t* test. (D) MOPC315.BM-Luc cells were cultured with the indicated concentrations of the anti-CD44 antibody Hermes-1 in the presence of HA under shear stress for 1 hour. The means ± SD (bars) of the size of cell clusters are shown (n = 8-20). *$P < .05$ by one-way ANOVA with Tukey's multiple comparison test. (E) MOPC315.BM-Luc cells were cultured with the indicated concentrations of control IgG or Hermes-1 (anti-CD44). Cell proliferation was assessed after 72 hours and is expressed as a percentage of the values for corresponding untreated cells. The means ± SD (bars) of 3 independent experiments are shown. (F) We intravenously transplanted 5 × 10^5 MOPC315.BM.Luc cells into BALB/c mice. Beginning 4 weeks after transplantation, mice were administered 10 mg/kg of isotype-matched immunoglobulin (IgG) or the anti-CD44 antibody Hermes-1 (Anti-CD44) along with 50 μg/kg HA twice a week for an additional 4 weeks.[38] Representative overlay photographs taken by the IVIS-CT Imaging System on Day 70 are shown with the location of the intramedullary tumors, splenic tumors, and EMD lesions. (G) The numbers of EMD lesions in each mouse were counted. The *P* value was determined by Student *t* test.

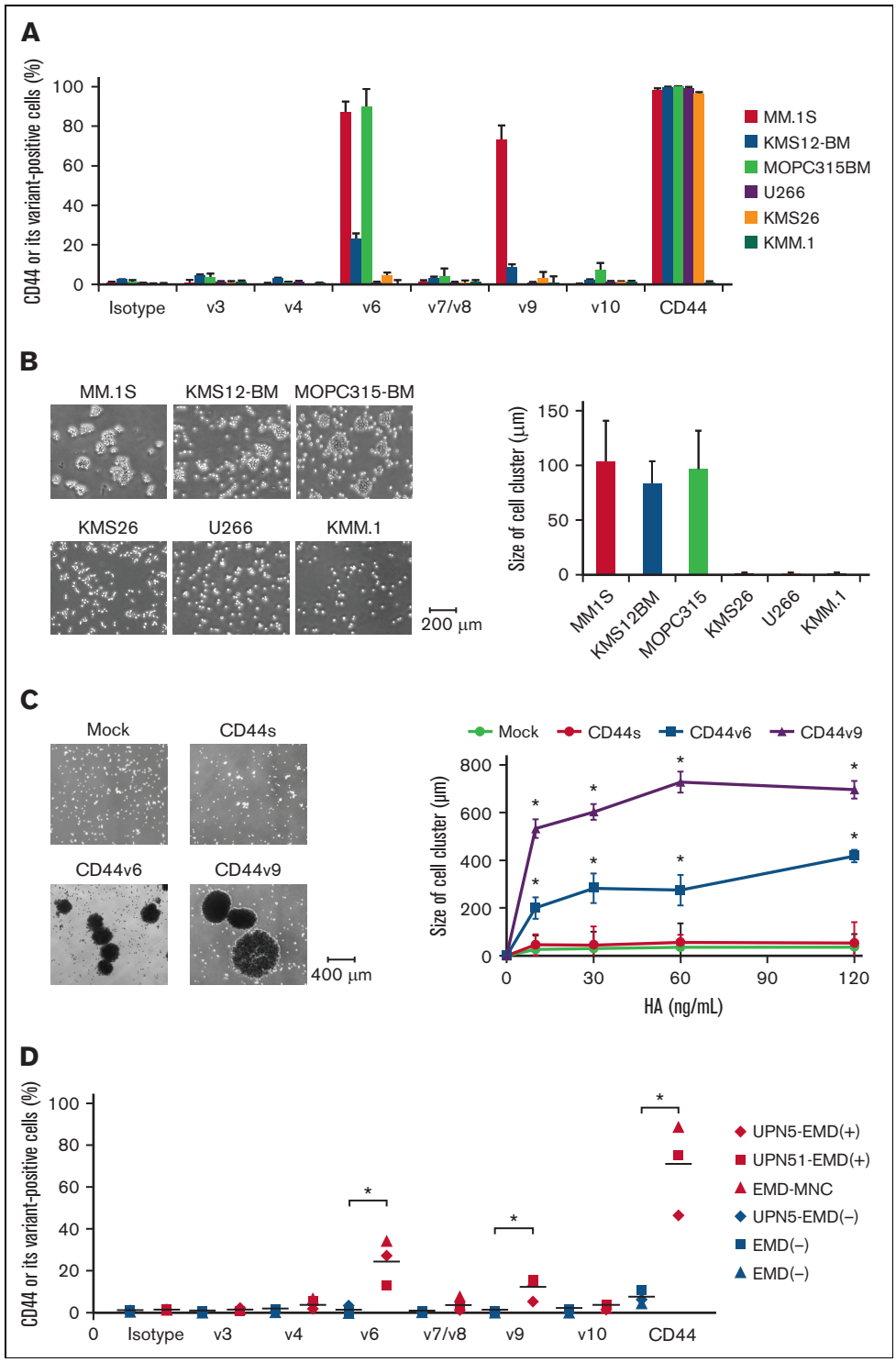

Figure 4. HA-induced cluster formation is dependent on the expression of long-stretch CD44 variants. (A) Flow cytometric analysis of the expression of CD44 and its variants on MM cell lines. The means ± SD (bars) of 3 independent experiments are shown. (B) MM cells were cultured at 1 × 10^5 cells/mL in the presence of 120 ng/mL of HA under shear stress for 1 hour. Left panel: Representative phase-contrast images of MM cells. Bar represents 200 μm. Right panel: The means ± SD (bars) of the size of the cell clusters (n = 8-20). (C) KMM.1 sublines were cultured at 1 × 10^5 cells/mL with the indicated concentrations of HA under shear stress for 1 hour. Left panel: Representative phase-contrast images of 4 KMM.1 sublines cultured with 120 ng/mL of HA. Bar represents 400 μm. Right panel: The means ± SD (bars) of the size of cell clusters (n = 8-20). *$P < .05$ by one-way ANOVA with Tukey's multiple comparison test. (D) Flow cytometric analysis of the expression of CD44 and its variants on primary MM cells isolated from the BM (except for EMD-MNC, which was isolated from the EMD lesion) of patients with (+) or without (–) EMD. In a patient with UPN5, BM samples were isolated at diagnosis [EMD (–)] and before the development of EMD [EMD (+)] (Supplemental Figure 2C). *$P < .05$ by one-way ANOVA with Tukey's multiple comparison test between EMD (+) and EMD (–) groups.

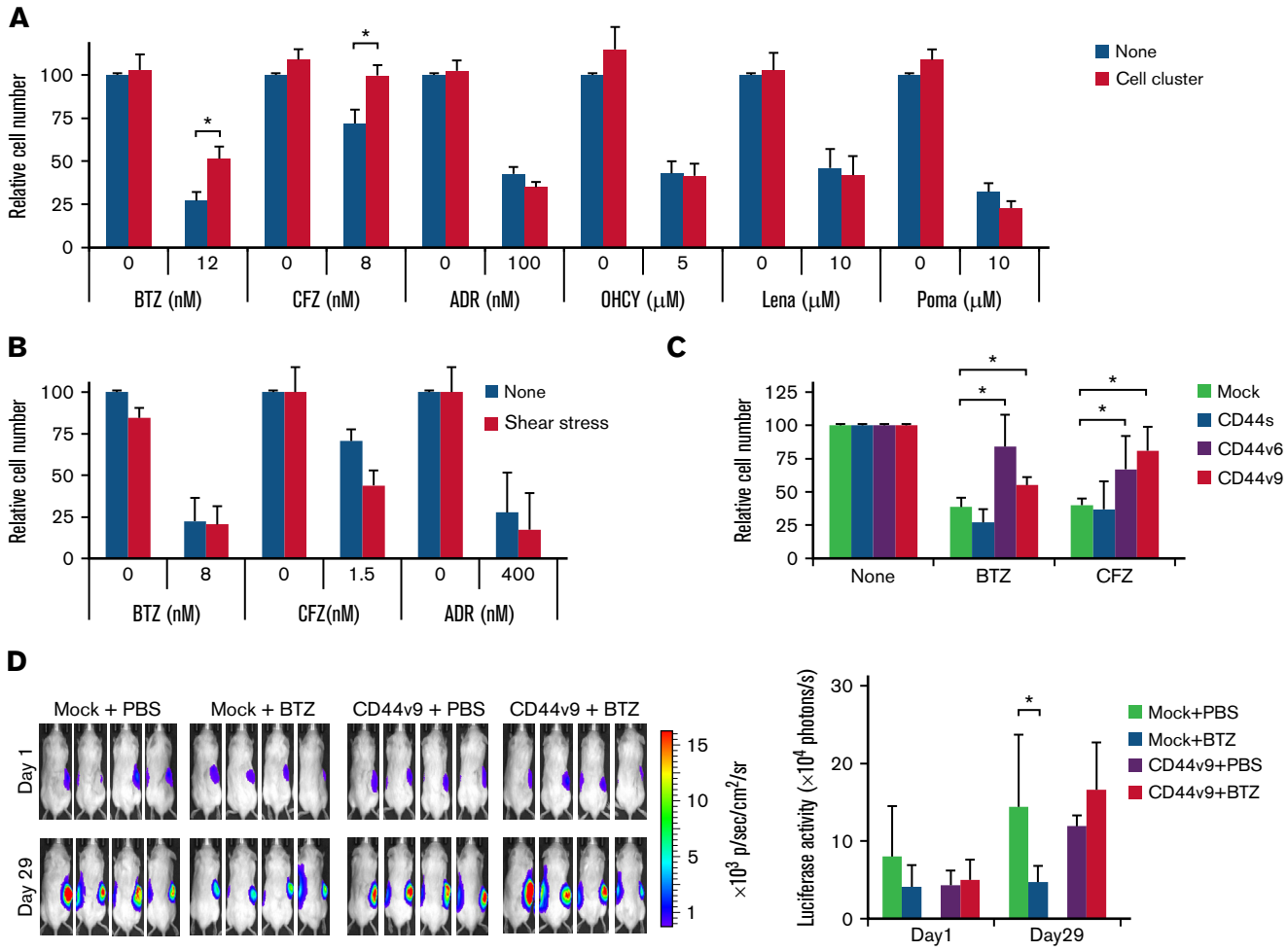

E

	BCJ 2017	MM.1S	KMS12-BM
SLC1A4	0.371	1.12	1.06
GLA	0.482	0.847	0.974
AKNA	0.247	1	1.22
ARHGAP27	0.278	0.98	0.912
LY96	0.263	0.909	0.918
MSL3	0.447	0.928	0.922
SQRDL	0.256	0.975	0.953
NCAPH2	0.47	1	1.001
MRI1	0.408	1.09	0.992
RAB8A	0.477	0.95	0.933
ABHD2	0.404	0.86	1.09
LMF2	0.391	1.1	0.838
TUBA4A	0.457	1	1.07
C2ORF69	0.491	0.96	1.03
PTPN18	0.38	1.05	1.03
PRKD2	0.286	1.04	0.995
KHK	0.403	0.998	0.932
CERK	0.403	0.983	0.903
GPSM3	0.188	0.986	0.985
WFS1	0.417	0.989	0.96
MYH9	0.497	1.055	1.025
CYTIP	0.35	1.02	0.994
SVIP	0.466	1.07	0.916
ARSA	0.303	0.926	1.03
SFMBT2	0.474	0.98	1.135

	BCJ 2017	MM.1S	KMS12-BM
NEK3	2.544	1.03	0.885
DLST	2.001	1.25	1.08
TARS2	2.083	1	0.978
C6ORF48	2.462	1.06	1.063
HSPA1B	2.335	1.22	1.08
TFEB	2.302	1.11	1.05
RNF170	2.34	1.12	1.16
SOX12	2.281	2.12	1.19
PAQR6	3.645	1.02	1.05
HIST1H2BD	4.514	0.976	1.07
UBE2K	2.048	0.956	0.94
LYSMD1	2.379	1.02	1.06
MNAT1	2.144	1.14	1.02
POLR3GL	2.251	1.03	0.928

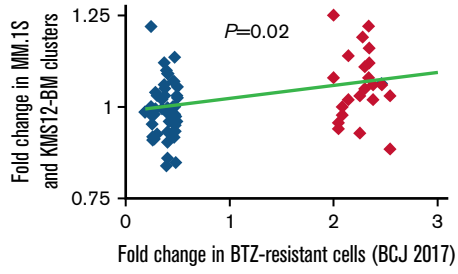

Figure 5.

mice (Figure 2D-E; supplemental Figure 3D-E). At autopsy, tumor masses were found in the liver, soft tissues, and skin in 9 of 10 HA-treated mice but none in vehicle-treated mice (Figure 2C-F and supplemental Figure 3F for data quantification). These masses were diagnosed as plasmacytomas by outside specialists of animal pathology (supplemental Figure 3E). Tumor cells were strongly aggregated and showed positive staining for HABP in the BM of HA-injected mice (Figure 2G). We detected aggregated MOPC cells as circulating tumor cells in the peripheral blood of recipient mice (supplemental Figure 3G). HA administration significantly shortened the survival of MOPC-transplanted mice but did not affect the survival of nontransplanted BALB/c mice (Figure 2B). The development of EMD appeared to be the major cause of shortened survival because HA did not confer a growth advantage to MOPC cells (supplemental Figure 3C).

To confirm that HA-induced EMD development is mediated via interaction of HA with CD44 on MM cells, we performed the same experiments using CD44-deleted MOPC sublines (Figure 3A; supplemental Figure 4A). As shown in Figure 3B-C, HA failed to generate EMD from CD44-null MM cells in vivo and did not shorten the survival of transplanted mice. Furthermore, we attempted to inhibit EMD generation in this model using an anti-CD44 antibody. The specific anti-CD44 antibody Hermes-1 significantly inhibited cell cluster formation at the concentrations >2.5 μg/mL (Figure 3D) without affecting cell growth in vitro (Figure 3E). To achieve this concentration, we treated HA-administered mice with 10 mg/kg of Hermes-1 or isotype-matched immunoglobulin (IgG2a) twice a week.[38] As anticipated, the anti-CD44 antibody significantly reduced the number of EMD lesions per mouse from 1.38 ± 0.74 to 0.50 ± 0.76 (P = .02191) (Figure 3F-G; supplemental Figure 4B).

CD44 variants v6 and v9 are involved in EMD development of MM

CD44 is a major HA receptor, and its alternatively spliced variants are involved in metastasis and other aggressive behaviors of cancer cells.[21-24] Previous studies indicated that CD44 variants, especially CD44v9, were highly expressed in EMD lesions, upregulated during disease progression, and negatively correlated with the prognosis of patients with MM.[18,25] However, no mechanistic insights have been described in these studies; therefore, we investigated the roles of CD44 variants in EMD development in our system. Among the 6 MM cell lines tested, MM.1S, KMS12-BM, and MOPC cells expressed CD44 variant v6 and/or v9 (Figure 4A) and formed large cell clusters in response to HA in vitro (Figure 4B). To confirm the correlation of CD44 variants and cluster formation, we transduced KMM.1 cells, which lack CD44 expression, with CD44v6 and CD44v9 expression vectors (supplemental Figure 4C). Although total CD44 expression was comparable among the sublines, the introduction of CD44v6 or CD44v9 generated significantly larger cell clusters than did mock- and CD44s-transduced KMM.1 cells (Figure 4C). In addition, CD44v6 and CD44v9 were exclusively detected in MM cells in the BM of EMD-positive patients (Figure 4D). Notably, CD44 variants were not detected at diagnosis but appeared just before the development of EMD in a patient who developed EMD during treatment (Figure 4D; supplemental Figure 2C). CD44 variants have additional stretches in the extracellular domain of CD44s, which might enhance cell–cell interactions to form larger cell clusters. This notion is consistent with previous reports that CD44v6 and CD44v9 are preferentially involved in cell–cell interactions rather than in cell–matrix interactions.[39]

Cell clusters acquire resistance to proteasome inhibitors via activation of CD44 signaling

EMD has been associated with chemoresistance and poor prognosis in patients with MM[10-12]; however, the underlying mechanisms of the development of drug resistance are not fully elucidated. To address this issue, we first examined the cytotoxic effect of various anti-MM drugs on cell clusters generated in cultures of MM cells with BMSC supernatants under shear stress. Shear stress-induced cluster formation conferred resistance to PIs, bortezomib and carfilzomib, to KMS12-BM (Figure 5A), and to MM.1S cells (supplemental Figure 5A). On the other hand, cell clusters retained their sensitivity to other therapeutic agents, such as doxorubicin, 4-hydroxycyclophosphamide, and immunomodulatory drugs (lenalidomide and pomalidomide), without affecting cluster formation (supplemental Figure 5B). PI resistance was fully reproduced in KMS12-BM and MM.1S cells cultured with HA, instead of with UBE6T-7 supernatants, under shear stress (supplemental Figure 5C). Cluster formation was essential for

Figure 5. Cell–cell homophilic interactions confer PI resistance to MM cells. (A) KMS12-BM cells were cultured with the indicated concentrations of bortezomib (BTZ), carfilzomib (CFZ), doxorubicin (ADR), 4-hydroxycyclophosphamide (OHCY), lenalidomide (Lena), or pomalidomide (Poma) in the presence of UBE6T-7 BMSC supernatants in the absence (None) or presence (Cell cluster) of shear stress exposure. Cell proliferation was assessed after 72 hours and is expressed as a percentage of the value for corresponding untreated cells without exposure to shear stress. *$P < .05$ determined by one-way ANOVA with the Student-Newman-Keuls multiple comparison test (n = 6-10). (B) The experiments described in A were carried out with non–cluster-forming RPMI8226 cells. (C) Mock-, CD44s-, CD44v6-, or CD44v9-transfected KMM.1 cells were cultured with suboptimal doses of bortezomib (BTZ) or carfilzomib (CFZ) along with 100 ng/mL of HA under shear stress. Cell proliferation was assessed after 72 hours and is expressed as a percentage of the value for corresponding drug-untreated cells. *$P < .05$ determined by one-way ANOVA with the Student-Newman-Keuls multiple comparison test (n = 6-10). (D) We subcutaneously inoculated 5×10^6 luciferase-expressing KMM.1-mock (Mock) or KMM.1-CD44v9 (CD44v9) cells in the right thigh of NOD/SCID mice. Mice were intraperitoneally administered vehicle alone (PBS) or 2 mg/kg bortezomib (BTZ) twice a week for 3 weeks. Treatments were started when tumor-derived luciferase activity was measurable, defined as Day 1. Left panel: Representative photographs of mice on Day 1 and Day 29 (original magnification, ×2). Right panel: Quantitative data of in vivo bioluminescence on Day 1 and Day 29 expressed as photon units (photons/s). The means ± SD (bars) are shown. *$P < .05$ by one-way ANOVA with Tukey's multiple comparison test (n = 4). (E) MM.1S and KMS12-BM cells were cultured at 1×10^5 cells/mL in the presence of UBE6T-7 supernatants with or without shear stress for 24 hours. Total RNA was isolated and subjected to microarray analysis for global changes in gene expression. The data have been deposited in the MIAME-compliant GEO database under accession number GSE189364. We selected the genes significantly downregulated (blue/sky blue) or upregulated (red/pink) in bortezomib-resistant primary MM cells in a previous study[40] (BCJ 2017) and compared their expression with that in MM.1S and KM12-BM cell clusters. The numbers indicate fold increases in the expression level of each gene in shear stress-induced cell clusters against nonclustered MM.1S and KM12-BM cells ($P = .02$ by Spearman's rank correlation).

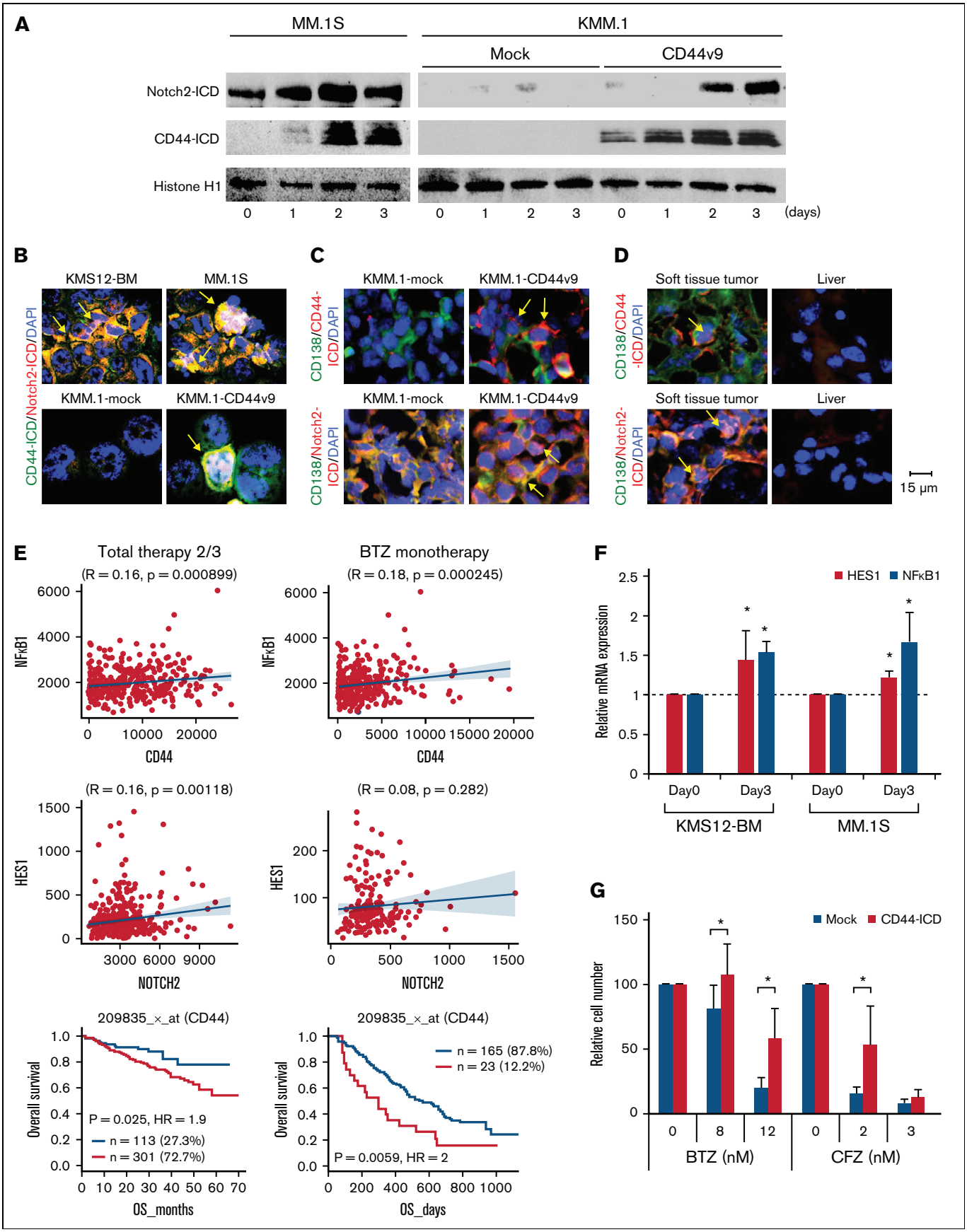

Figure 6.

PI resistance because non–cluster-forming RPMI8226 cells succumbed to PIs under the same conditions (Figure 5B), and MM.1S cells were sensitive to PIs under shear stress in the absence of HA (supplemental Figure 5D).

Next, we investigated the role of CD44 variants in PI resistance of MM cell clusters. Exogenous expression of either CD44v6 or CD44v9, but not CD44s, resulted in the acquisition of PI resistance in CD44^{-} KMM.1 cells in vitro (Figure 5C; supplemental Figure 4C). In a murine xenograft model, CD44v9-transduced KMM.1 cells (KMM.1-CD44v9) were obviously resistant to bortezomib treatment, while the growth of mock-transfected KMM.1 cells was significantly suppressed by bortezomib (Figure 5D). Gene expression profiling revealed the enrichment of PI resistance-associated genes, which were identified by unbiased screening in patients with MM,[40] in KMS12-BM- and MM.1S-derived cell clusters compared with parental nonclustered cells (Figure 5E). These results suggest that CD44-mediated transcriptional changes promote PI resistance in MM cell clusters.

It has been reported that CD44 is cleaved by γ-secretase and that the liberated intracellular domain of CD44 (CD44-ICD) translocates into the nucleus, where it acts as a transcriptional activator to mediate drug resistance in solid tumors.[41] Similarly, Notch-mediated signals promote PI resistance via γ-secretase–induced cleavage of the Notch-ICD in MM cells,[42] in which Notch2 is ubiquitously and highly expressed among Notch family members.[43] Furthermore, Lin et al[44] reported the role of interleukin-6–mediated crosstalk between CD44 and Notch in stroma-instructive tumorigenesis. We therefore monitored the levels of CD44-ICD and Notch2-ICD during HA-induced cluster formation of MM.1S and KMM.1-CD44v9 cells. Immunoblot analyses of nuclear extracts revealed that the expression levels of CD44-ICD and Notch2-ICD appreciably increased in cell clusters of MM.1S and KMM.1-CD44v9 but not those derived from KMM.1-mock cells in a time-dependent manner (Figure 6A). Nuclear localization of CD44-ICD and Notch2-ICD was demonstrated by immunofluorescent staining in cell clusters derived from KMS12-BM, MM.1S, and KMM.1-CD44v9 cells (Figure 6B). We obtained virtually identical results in the histopathological analyses of KMM.1-CD44v9 cells inoculated in immunodeficient mice (Figure 6C) and the EMD lesions in MOPC cell-transplanted BALB/c mice (Figure 6D). In addition, the expression of HES1 and NF-kB1, which are downstream targets of CD44-ICD and Notch-ICD[45,46] (Figure 6E), was significantly upregulated in MM cell clusters (Figure 6F). Finally, ectopic expression of CD44-ICD significantly decreased the sensitivity of CD44^{-} KMM.1 cells to PIs (Figure 6G; supplemental Figure 5E). These results are compatible with the negative prognostic impact of CD44 expression on patients with MM treated with bortezomib-based regimens (Figure 6E, lowermost panel).

Targeting CD44 signaling overcomes cell cluster-mediated PI resistance in MM cells

The above notion prompted us to hypothesize that γ-secretase inhibitors (GSIs) overcome PI resistance in EMD by interfering with the liberation of CD44-ICD and/or Notch2-ICD. To corroborate this hypothesis, we first confirmed a dose-dependent decline in CD44-ICD and Notch2-ICD expression levels in response to the γ-secretase inhibitor GSI-XII (Z-IL-CHO) in HA-induced cell clusters of MM.1S (Figure 7A). Before γ-secretase–mediated generation of ICD, extracellular domains should be removed by the aid of matrix metalloproteinases (MMP), such as MMP9 and MMP13, for CD44 and tumor necrosis factor-α–converting enzyme for Notch2.[41] Consistent with this notion, an MMP9/13 inhibitor cancelled the generation of CD44-ICD but not Notch2-ICD in MM cell clusters (Figure 7A). In parallel with the suppression of CD44-ICD, both inhibitors significantly increased the sensitivity of cell clusters to bortezomib and exerted an additive cytotoxic effect with bortezomib on MM cell clusters (Figure 7B). Next, we attempted to validate the effect of GSI on overcoming CD44 variant-mediated bortezomib resistance in a murine xenograft model. To this end, we inoculated KMM.1-CD44v9 cells subcutaneously into immunodeficient mice and treated the mice with vehicle alone, bortezomib alone, GSI-XII alone, or the combination of bortezomib and GSI-XII (GSI-XII first and then bortezomib) twice a week for 3 weeks. As anticipated, administration of bortezomib alone did not significantly inhibit the growth of PI-resistant KMM.1-CD44v9 cells at the dose and schedule used in this experiment (Figure 7C). GSI alone also failed to retard the growth of KMM.1-CD44v9 xenografts but almost completely cancelled the resistance to bortezomib in vivo (Figure 7C). As shown in Figure 7D, 20 nM of bortezomib suppressed the growth of HA-treated MOPC cells by ~40% of untreated controls under shear stress, whereas approximately 80% of bortezomib-treated MOPC cells underwent apoptosis in the

Figure 6. MM cell clusters acquire PI resistance via activation of CD44 signaling. (A) We cultured MM.1S, KMM.1-mock and KMM.1-CD44v9 cells in the presence of 500 ng/mL of HA under shear stress for the indicated periods and isolated nuclear extracts for immunoblot analysis for the expression of Notch2-ICD, CD44-ICD and histone H1 (internal control). (B) Cytospin specimens were prepared during the experiments described in A for immunocytochemical staining with anti-CD44 and anti-Notch2 antibodies, followed by the staining with Alexa Fluor 488-conjugated anti-mouse IgG (green) and Alexa Fluor 594-conjugated anti-rabbit IgG (red). (C) Tumor sections were obtained from mice described in Figure 5D and stained with FITC-conjugated anti-CD138 (green) and anti-CD44 or anti-Notch2, followed by the staining with Alexa Fluor 594-conjugated anti-rabbit IgG (red). (D) Histological sections were prepared from soft tissue tumors and livers of MOPC-transplanted BALB/c mice (Figure 2F) and stained with FITC-conjugated anti-mouse CD138 (green) and anti-mouse CD44 or anti-mouse Notch2, followed by the staining with Alexa Fluor 594-conjugated anti-rabbit IgG (red). Nuclei were counterstained with DAPI (blue). Bar represents 15 μm. (E) We examined the correlation between the expression of CD44 and its effectors and the prognostic impact of CD44 using DNA microarray data from patients with MM treated with Total Therapy 2/3 (GEO accession number GSE4581) or bortezomib monotherapy[54] (BTZ monotherapy) with the GenomicScape tool (www.genomicscape.com). Upper and middle panels: Correlation between CD44 and NFkB1 or between Notch2 and HES1. Lower panels: Kaplan-Meier curves of patients with MM with high (red) and low (blue) CD44 expression. *P* values and the hazard ratio (HR) were determined by the log-rank test. (F) KMS12-BM and MM.1S cells were cultured with HA under shear stress for the indicated periods and subjected to quantitative reverse transcription-PCR for downstream CD44 effectors. Data were quantified by the $2^{-\Delta\Delta Ct}$ method using *GAPDH* as a reference gene and are shown as the fold increase against the values for Day 0. (G) Mock- or CD44-ICD-transfected KMM.1 cells were cultured with the indicated concentrations of bortezomib or carfilzomib. Cell proliferation was assessed after 72 hours and is expressed as a percentage of the value for corresponding untreated cells. *$P < .05$ determined by one-way ANOVA with the Student-Newman-Keuls multiple comparison test (n = 6-10).

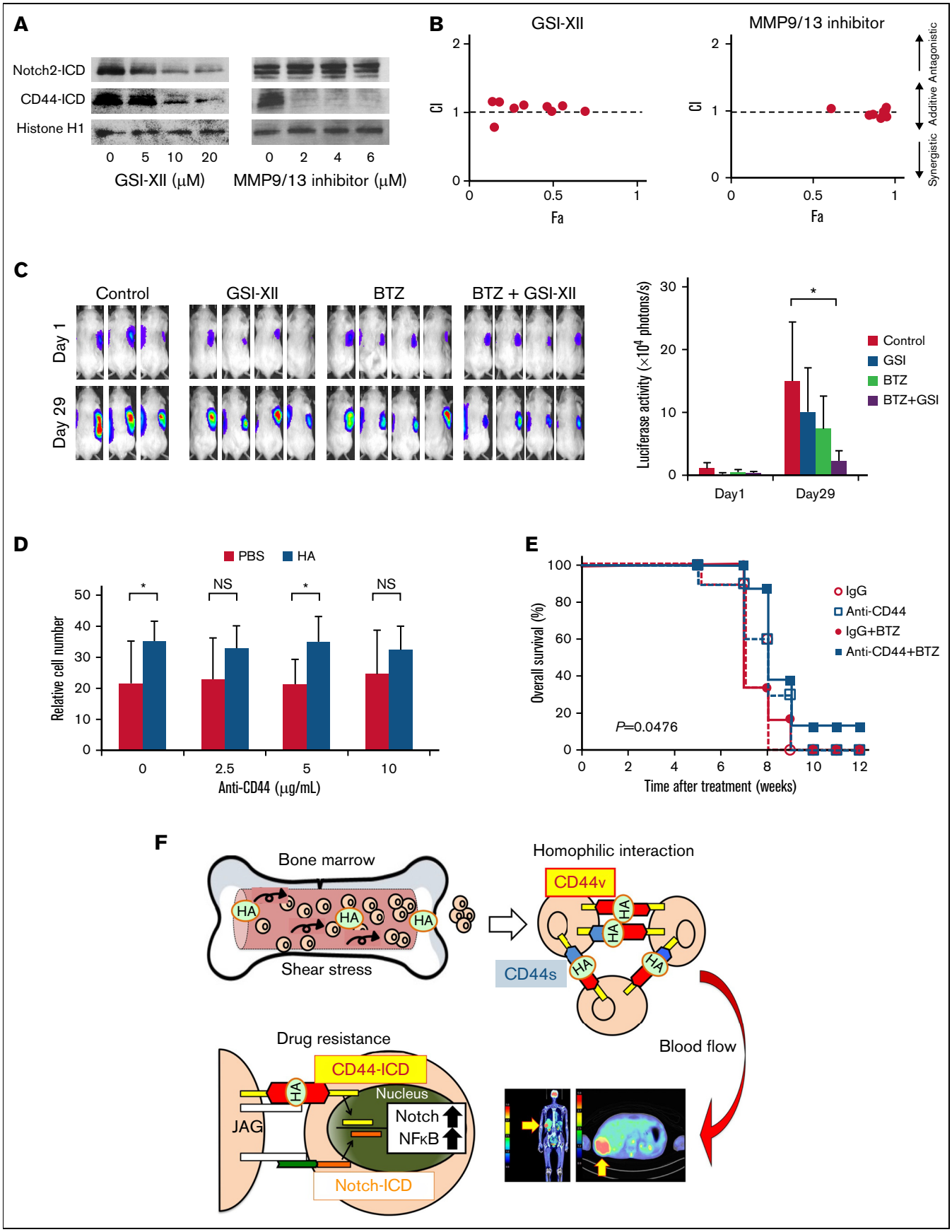

Figure 7.

absence of HA (PBS group). The resistance of HA-induced MOPC cell clusters to bortezomib was nearly abrogated by 10 μg/mL of anti-CD44 antibody in vitro (Figure 7D). Furthermore, the anti-CD44 antibody enhanced the therapeutic effects of bortezomib and significantly prolonged the survival of HA-treated/MOPC-transplanted BALB/c mice (Figure 7E). These results imply that targeting CD44 signaling with GSIs or an anti-CD44 antibody could overcome PI resistance of EMD in patients with MM.

Discussion

In the present study, we show that homophilic cell–cell interactions of MM cells are induced by HA under shear stress via the surface HA-CD44 complex as a linker, which might represent an origin of EMD (Figure 7F). This conclusion is supported by clinical observations that (1) serum HA concentrations were significantly higher in patients with MM with EMD than in patients without EMD and (2) CD44 variants were highly expressed in MM cells derived from EMD lesions.[25] Cell cluster formation confers PI resistance via γ-secretase–mediated activation of CD44-ICD, which provides potential therapeutic targets for patients with MM with EMD. As a proof of concept, we demonstrated that PI resistance was reversed by GSI or anti-CD44 antibody in vitro and in vivo. Future clinical application of CD44-targeting agents may increase the therapeutic index of standard-of-care regimens and improve the currently dismal prognosis of patients with MM with EMD.

The binding of HA to surface CD44 triggers the homophilic interaction of MM cells, which is enhanced by physiological shear stress in the BM microenvironment to serve as a seed of EMD. We identified BMSCs but not MM cells as the source of HA because HA synthetases were expressed only in BMSCs. This is compatible with a previous report that HA was mainly synthesized by HAS3 in BMSCs in healthy individuals.[47] However, it has been demonstrated that HAS1 expression was specifically detected in BMSCs of patients with MM and was upregulated by proinflammatory cytokines in inflammatory states.[48] In addition, the inflammatory marker C-reactive protein was significantly elevated in patients with MM with EMD compared with patients without EMD.[6] Inflammation may play a causative role in higher serum concentrations of HA in patients with MM with EMD.

Murine models are useful for analyzing the mechanisms of EMD emergence and testing novel treatment strategies for EMD.[20,31] Using a transplantable CD44-expressing MM cell line, we show that the administration of HA could induce EMD lesions in the liver and skin/soft tissues in a murine syngeneic model that faithfully reproduces human EMD. On the other hand, Roccaro et al[20] induced EMD in the liver, kidney, and pelvic region by adopting a serial in vivo selection in mice transplanted with liver-prone MM.1S cells. They suggested that EMD development is regulated by increases in epithelial mesenchymal transition–like transcriptional activity, which leads to higher CXCR4 expression. Alterations in distinct molecules may cause different patterns of EMD in murine models and probably in patients with MM.

Relatively little is known about the signaling pathways of EMD-causative surface molecules, such as CD44 and CXCR4, and the downstream effector genes responsible for EMD development. Long noncoding RNAs (lncRNAs) are involved in crucial biological functions such as gene expression, chromatin reorganization, and cell differentiation. According to a recent report, lncRNAs account for 82% of the transcriptome in MM cells and are more heterogeneously expressed than protein-coding genes.[49] Among the known MM-related lncRNAs, *metastasis associated lung adenocarcinoma 1* (*MALAT1*) plays critical roles in the enhancement of cell growth, metastasis, and disease progression via transactivation of CD44 and other metastasis-related genes in lung cancer.[50] *MALAT1* was also identified as a poor prognostic factor and an inducer of disease progression via inhibition of apoptosis as well as enhancement of cell growth and glycolysis in MM cells.[51-53] In particular, Handa et al[52] reported that *MALAT1* expression was markedly higher in EMD-derived MM cells than in corresponding intramedullary cells. Consistent with this observation, *MALAT1* expression was readily upregulated during HA-induced cell cluster formation of MM.1S cells under shear stress (supplemental Figure 5F). Given the high expression of CD44 in EMD lesions[18] and circulating MM cells,[37] it can be speculated that *MALAT1* is involved in CD44 upregulation in EMD.

Several clinical studies indicate that the presence of high-risk cytogenetics as well as low hemoglobin levels and/or platelet counts at diagnosis are associated with an increased risk of EMD relapse[6-13];

Figure 7. Targeting CD44 signaling overcomes cluster-mediated PI resistance in MM cells. (A) MM.1S cells were cultured with 500 ng/mL of HA under shear stress for 24 hours in the presence of GSI-XII or an MMP9/13 inhibitor at the indicated concentrations. Nuclear extracts were subjected to immunoblotting for the expression of Notch2-ICD, CD44-ICD, and histone H1 (internal control). (B) MM.1S cells were cultured with 500 ng/mL of HA under shear stress and treated with bortezomib in combination with GSI-XII or an MMP9/13 inhibitor for 72 hours. Dose-response curves of each combination were generated to make nonconstant normalized isobolograms at IC_{50} using CompuSyn software.[15] The isobolograms shown are representative of at least 3 independent experiments. A combination index (CI) <1.0 indicates the synergism of the 2 drugs. (C) We subcutaneously inoculated 5×10^6 luciferase-expressing KMM.1-CD44v9 cells into the right thigh of NOD/SCID mice. When inoculated tumors were palpable (Day 1), mice were randomly assigned to 4 arms of treatment with intraperitoneal injection of vehicle alone (Control), 2 mg/kg of GSI-XII, 2 mg/kg of bortezomib, or GSI-XII plus bortezomib (GSI-XII first, followed by bortezomib) twice a week for 3 weeks. Left panel: Representative photographs of mice on Day 1 and Day 29 (original magnification, ×2). Right panel: Quantitative data of in vivo bioluminescence imaging on Day 1 and Day 29 expressed as photon units (photons/s). The means ± SD (bars) are shown. *$P < .05$ by one-way ANOVA with Tukey's multiple comparison test (n = 4). (D) MOPC cells were cultured with bortezomib (20 nM) in the presence of vehicle (PBS) or 500 ng/mL of HA under shear stress along with the indicated concentrations of anti-CD44 antibody. Cell proliferation was assessed after 72 hours and is expressed as a percentage of the value for corresponding untreated cells. *$P < .05$ determined by one-way ANOVA with the Student-Newman-Keuls multiple comparison test (n = 3). (E) We intravenously injected 5×10^5 luciferase-expressing MOPC315.BM.Luc cells into BALB/c mice. Four weeks after transplantation, mice were injected with 50 μg/kg of HA and treated with intraperitoneal administration of isotype-matched immunoglobulin (IgG), anti-CD44 antibody (anti-CD44), IgG plus bortezomib (IgG + BTZ), or anti-CD44 antibody plus bortezomib (anti-CD44 + BTZ) (IgG or anti-CD44 antibody first, followed by bortezomib) twice a week for an additional 4 weeks. Kaplan-Meier survival curves are shown. *P* value was determined between the anti-CD44 + BTZ group and the IgG + BTZ group by the log-rank test. (F) Graphic abstract. See Results and Discussion for details.

however, risk factors for EMD development have not yet been defined. The present study suggests that high serum concentrations of HA and increased expression of CD44 variants can predict the development of EMD; however, the sample size of our clinical study is too small to draw a firm conclusion. We therefore propose to initiate a prospective study with a larger cohort to better define the predictive power of the 2 parameters.

Acknowledgments

The authors are grateful to Akiko Yonekura, Mayuka Shiino (Jichi Medical University), and Tomoko Hishima (International Myeloma Center for Advanced Research and Treatment) for their technical assistance. The authors are indebted to Akihiro Umezawa (National Research Institute for Child Health and Development, Tokyo, Japan) and Hirofumi Hamada (Sapporo Medical University, Sapporo, Japan) for providing UBE6T-7 and stroma-NK cell lines, respectively.

This work was supported by a Grant-in-Aid for Scientific Research from Japan Society for Promotion of Science (J.K. and Y.F.) and the Bristol-Myers Squibb Research Grant (Y.F.); the Japan Leukemia Research Fund, Yasuda Memorial Cancer Foundation, Takeda Science Foundation, and Novartis Foundation Japan (J.K. and Y.F.); the Mitsui Life Social Welfare Foundation, SENSHIN Medical Research Foundation, and Princess Takamatsu Cancer Research Fund (J.K.); the Kano Foundation Research Grant and the International Myeloma Foundation Japan's Grant (J.K.).

Authorship

Contribution: J.K. performed the experiments, analyzed the data, and drafted the manuscript; N.O. and Y.K. performed the experiments; N.K., M.T., S.I., T.K., Y.K., M.U., N.T., and A.M. provided clinical data and samples; B.B. and H.Y. provided the cell lines; Y.F. designed and supervised the research and finalized the manuscript; and all authors approved the manuscript before submission.

Conflict-of-interest disclosure: The authors declare no competing financial interests.

ORCID profiles: N.K., 0000-0002-5279-029X; M.T., 0000-0003-2140-4007; T.K., 0000-0002-9914-7517; H.Y., 0000-0003-0905-6855; N.T., 0000-0002-6758-3787; Y.F., 0000-0002-7249-6418.

Correspondence: Yusuke Furukawa, Division of Stem Cell Regulation, Center for Molecular Medicine, Jichi Medical University, 3311-1 Yakushiji, Shimotsuke, Tochigi 329-0498, Japan; email: furuyu@jichi.ac.jp.

References

1. Siegel RL, Miller KD, Fuchs HE, Jemal A. Cancer Statistics, 2021. *CA Cancer J Clin*. 2021;71(1):7-33.
2. Owens B. Outlook: multiple myeloma. *Nature*. 2020;587(7835):S55.
3. Kumar SK, Rajkumar V, Kyle RA, et al. Multiple myeloma. *Nat Rev Dis Primers*. 2017;3(1):17046.
4. Furukawa Y, Kikuchi J. Molecular basis of clonal evolution in multiple myeloma. *Int J Hematol*. 2020;111(4):496-511.
5. Oshima K, Kanda Y, Nannya Y, et al. Clinical and pathologic findings in 52 consecutively autopsied cases with multiple myeloma. *Am J Hematol*. 2001;67(1):1-5.
6. Avivi I, Cohen YC, Suska A, et al. Hematogenous extramedullary relapse in multiple myeloma: a multicenter retrospective study in 127 patients. *Am J Hematol*. 2019;94(10):1132-1140.
7. Bansal R, Rakshit S, Kumar S. Extramedullary disease in multiple myeloma. *Blood Cancer J*. 2021;11(9):161.
8. Wu P, Davies FE, Boyd K, et al. The impact of extramedullary disease at presentation on the outcome of myeloma. *Leuk Lymphoma*. 2009;50(2):230-235.
9. Varettoni M, Corso A, Pica G, Mangiacavalli S, Pascutto C, Lazzarino M. Incidence, presenting features and outcome of extramedullary disease in multiple myeloma: a longitudinal study on 1003 consecutive patients. *Ann Oncol*. 2010;21(2):325-330.
10. Pour L, Sevcikova S, Greslikova H, et al. Soft-tissue extramedullary multiple myeloma prognosis is significantly worse in comparison to bone-related extramedullary relapse. *Haematologica*. 2014;99(2):360-364.
11. Bhutani M, Foureau DM, Atrash S, Voorhees PM, Usmani SZ. Extramedullary multiple myeloma. *Leukemia*. 2020;34(1):1-20.
12. Rosiñol L, Beksac M, Zamagni E, et al. Expert review on soft-tissue plasmacytomas in multiple myeloma: definition, disease assessment and treatment considerations. *Br J Haematol*. 2021;194(3):496-507.
13. Sklavenitis-Pistofidis R, Haradhvala NJ, Getz G, Ghobrial IM. Inflammatory stromal cells in the myeloma microenvironment. *Nat Immunol*. 2021;22(6):677-678.
14. Noborio-Hatano K, Kikuchi J, Takatoku M, et al. Bortezomib overcomes cell-adhesion-mediated drug resistance through downregulation of VLA-4 expression in multiple myeloma. *Oncogene*. 2009;28(2):231-242.
15. Kikuchi J, Koyama D, Wada T, et al. Phosphorylation-mediated EZH2 inactivation promotes drug resistance in multiple myeloma. *J Clin Invest*. 2015;125(12):4375-4390.
16. Kikuchi J, Kuroda Y, Koyama D, et al. Myeloma cells are activated in bone marrow microenvironment by the CD180/MD-1 complex which senses lipopolysaccharide. *Cancer Res*. 2018;78(7):1766-1778.
17. Kikuchi J, Hori M, Iha H, et al. Soluble SLAMF7 promotes the growth of myeloma cells via homophilic interaction with surface SLAMF7. *Leukemia*. 2020;34(1):180-195.

18. Dahl IM, Rasmussen T, Kauric G, Husebekk A. Differential expression of CD56 and CD44 in the evolution of extramedullary myeloma. *Br J Haematol*. 2002;116(2):273-277.
19. Azab AK, Quang P, Azab F, et al. P-selectin glycoprotein ligand regulates the interaction of multiple myeloma cells with the bone marrow microenvironment. *Blood*. 2012;119(6):1468-1478.
20. Roccaro AM, Mishima Y, Sacco A, et al. CXCR4 regulates extra-medullary myeloma through epithelial-mesenchymal-transition-like transcriptional activation. *Cell Rep*. 2015;12(4):622-635.
21. Mackay CR, Terpe HJ, Stauder R, Marston WL, Stark H, Günthert U. Expression and modulation of CD44 variant isoforms in humans. *J Cell Biol*. 1994; 124(1-2):71-82.
22. Mohamadzadeh M, DeGrendele H, Arizpe H, Estess P, Siegelman M. Proinflammatory stimuli regulate endothelial hyaluronan expression and CD44/ HA-dependent primary adhesion. *J Clin Invest*. 1998;101(1):97-108.
23. Ishimoto T, Nagano O, Yae T, et al. CD44 variant regulates redox status in cancer cells by stabilizing the xCT subunit of system xc(-) and thereby promotes tumor growth. *Cancer Cell*. 2011;19(3):387-400.
24. Liu X, Taftaf R, Kawaguchi M, et al. Homophilic CD44 interactions mediate tumor cell aggregation and polyclonal metastasis in patient-derived breast cancer models. *Cancer Discov*. 2019;9(1):96-113.
25. Eisterer W, Bechter O, Hilbe W, et al. CD44 isoforms are differentially regulated in plasma cell dyscrasias and CD44v9 represents a new independent prognostic parameter in multiple myeloma. *Leuk Res*. 2001;25(12):1051-1057.
26. Weinstock M, Aljawai Y, Morgan EA, et al. Incidence and clinical features of extramedullary multiple myeloma in patients who underwent stem cell transplantation. *Br J Haematol*. 2015;169(6):851-858.
27. Dahl IM, Turesson I, Holmberg E, Lilja K. Serum hyaluronan in patients with multiple myeloma: correlation with survival and Ig concentration. *Blood*. 1999;93(12):4144-4148.
28. Mori T, Kiyono T, Imabayashi H, et al. Combination of hTERT and bmi-1, E6, or E7 induces prolongation of the life span of bone marrow stromal cells from an elderly donor without affecting their neurogenic potential. *Mol Cell Biol*. 2005;25(12):5183-5195.
29. Kawano Y, Kobune M, Yamaguchi M, et al. Ex vivo expansion of human umbilical cord hematopoietic progenitor cells using a coculture system with human telomerase catalytic subunit (hTERT)-transfected human stromal cells. *Blood*. 2003;101(2):532-540.
30. Hofgaard PO, Jodal HC, Bommert K, et al. A novel mouse model for multiple myeloma (MOPC315.BM) that allows noninvasive spatiotemporal detection of osteolytic disease. *PLoS One*. 2012;7(12):e51892.
31. Ghobrial IM. Myeloma as a model for the process of metastasis: implications for therapy. *Blood*. 2012;120(1):20-30.
32. Slack SM, Cui Y, Turitto VT. The effects of flow on blood coagulation and thrombosis. *Thromb Haemost*. 1993;70(1):129-134.
33. Porat Z, Yaron I, Katz BZ, Kam Z, Geiger B. Shear flow-induced formation of tubular cell protrusions in multiple myeloma cells. *J Cell Physiol*. 2011; 226(12):3197-3207.
34. Bajorath J, Greenfield B, Munro SB, Day AJ, Aruffo A. Identification of CD44 residues important for hyaluronan binding and delineation of the binding site. *J Biol Chem*. 1998;273(1):338-343.
35. Osada N, Kikuchi J, Umehara T, et al. Lysine-specific demethylase 1 inhibitors prevent teratoma development from human induced pluripotent stem cells. *Oncotarget*. 2018;9(5):6450-6462.
36. Gkountela S, Castro-Giner F, Szczerba BM, et al. Circulating tumor cell clustering shapes DNA methylation to enable metastasis seeding. *Cell*. 2019; 176(1-2):98-112.e14.
37. Garcés JJ, Simicek M, Vicari M, et al. Transcriptional profiling of circulating tumor cells in multiple myeloma: a new model to understand disease dissemination. *Leukemia*. 2020;34(2):589-603.
38. Osawa Y, Kawai H, Tsunoda T, et al. Cluster of differentiation 44 promotes liver fibrosis and serves as a biomarker in congestive hepatopathy. *Hepatol Commun*. 2021;5(8):1437-1447.
39. Van Driel M, Günthert U, van Kessel AC, et al. CD44 variant isoforms are involved in plasma cell adhesion to bone marrow stromal cells. *Leukemia*. 2002;16(1):135-143.
40. Mitra AK, Harding T, Mukherjee UK, et al. A gene expression signature distinguishes innate response and resistance to proteasome inhibitors in multiple myeloma. *Blood Cancer J*. 2017;7(6):e581.
41. Nagano O, Saya H. Mechanism and biological significance of CD44 cleavage. *Cancer Sci*. 2004;95(12):930-935.
42. Muguruma Y, Yahata T, Warita T, et al. Jagged1-induced Notch activation contributes to the acquisition of bortezomib resistance in myeloma cells. *Blood Cancer J*. 2017;7(12):650.
43. Ishibashi M, Ueda K, Imai Y, Inokuchi K, Morita R, Tamura H. Notch1-JAG1 signaling induces aggressive myeloma cell behaviors. *Int. J. Myeloma*. 2020; 10:1-7.
44. Lin JT, Wang JY, Chen MK, et al. Colon cancer mesenchymal stem cells modulate the tumorigenicity of colon cancer through interleukin 6. *Exp Cell Res*. 2013;319(14):2216-2229.
45. Espinosa L, Cathelin S, D'Altri T, et al. The Notch/Hes1 pathway sustains NF-κB activation through CYLD repression in T cell leukemia. *Cancer Cell*. 2010;18(3):268-281.

46. García-Peydró M, Fuentes P, Mosquera M, et al. The NOTCH1/CD44 axis drives pathogenesis in a T cell acute lymphoblastic leukemia model. *J Clin Invest*. 2018;128(7):2802-2818.

47. Siiskonen H, Oikari S, Pasonen-Seppänen S, Rilla K. Hyaluronan synthase 1: a mysterious enzyme with unexpected functions. *Front Immunol*. 2015;6:43.

48. Calabro A, Oken MM, Hascall VC, Masellis AM. Characterization of hyaluronan synthase expression and hyaluronan synthesis in bone marrow mesenchymal progenitor cells: predominant expression of HAS1 mRNA and up-regulated hyaluronan synthesis in bone marrow cells derived from multiple myeloma patients. *Blood*. 2002;100(7):2578-2585.

49. Carrasco-Leon A, Ezponda T, Meydan C, et al. Characterization of complete lncRNAs transcriptome reveals the functional and clinical impact of lncRNAs in multiple myeloma. *Leukemia*. 2021;35(5):1438-1450.

50. Gutschner T, Hämmerle M, Eissmann M, et al. The noncoding RNA MALAT1 is a critical regulator of the metastasis phenotype of lung cancer cells. *Cancer Res*. 2013;73(3):1180-1189.

51. Cho SF, Chang YC, Chang CS, et al. MALAT1 long non-coding RNA is overexpressed in multiple myeloma and may serve as a marker to predict disease progression. *BMC Cancer*. 2014;14(1):809.

52. Handa H, Kuroda Y, Kimura K, et al. Long non-coding RNA MALAT1 is an inducible stress response gene associated with extramedullary spread and poor prognosis of multiple myeloma. *Br J Haematol*. 2017;179(3):449-460.

53. Ikeda S, Kitadate A, Abe F, Takahashi N, Tagawa H. Hypoxia-inducible KDM3A addiction in multiple myeloma. *Blood Adv*. 2018;2(4):323-334.

54. Mulligan G, Mitsiades C, Bryant B, et al. Gene expression profiling and correlation with outcome in clinical trials of the proteasome inhibitor bortezomib. *Blood*. 2007;109(8):3177-3188.